Available online at www.sciencedirect.com
ScienceDirect
Cellular Signalling xx (2006) xxx–xxx
CELLULAR SIGNALLING
www.elsevier.com/locate/cellsig

MAGI-3 regulates LPA-induced activation of Erk and RhoA

Huanchun Zhang [a], Dongsheng Wang [a], Hong Sun [a], Randy A. Hall [b], C. Chris Yun [a,c,*]

[a] Department of Medicine, Emory University School of Medicine, Atlanta, GA 30322, USA
[b] Department of Pharmacology, Emory University School of Medicine, Atlanta, GA 30322, USA
[c] Department of Physiology, Emory University School of Medicine, Atlanta, GA 30322, USA

Received 30 May 2006; accepted 29 June 2006

Abstract

Lysophosphatidic acids (LPA) exert multiple biological effects through specific G protein-coupled receptors. The LPA-activated receptor subtype LPA_2 contains a carboxyl-terminal motif that allows interaction with PDZ domain-containing proteins, such as NHERF2 and PDZ-RhoGEF. To identify additional interacting partners of LPA_2, the LPA_2 carboxyl-terminus was used to screen a proteomic array of PDZ domains. In addition to the previously identified NHERF2, several additional LPA_2-interacting PDZ domains were found. These included MAGI-2, MAGI-3 and neurabin. In the present work, we demonstrate the specific interaction between LPA_2 and MAGI-3, and the effects of MAGI-3 in colon cancer cells using SW480 as a cell model. MAGI-3 specifically bound to LPA_2, but not to LPA_1 and LPA_3. This interaction was mediated via the fifth PDZ domain of MAGI-3 interacting with the carboxyl-terminal 4 amino acids of LPA_2, and mutational alteration of the carboxyl-terminal sequences of LPA_2 severely attenuated its ability to bind MAGI-3. LPA_2 also associated with MAGI-3 in cells as determined by co-affinity purification. Overexpression of MAGI-3 in SW480 cells showed no apparent effect on LPA-induced activation of Erk and Akt. In contrast, silencing of MAGI-3 expression by siRNA drastically inhibited LPA-induced Erk activation, suggesting that the lack of an effect by overexpression was due to the high endogenous MAGI-3 level in these cells. Previous studies have shown that the cellular signaling elicited by LPA results in activation of the small GTPase RhoA by $G\alpha_{12/13}$ — as well as $G\alpha_q$-dependent pathways. Overexpression of MAGI-3 stimulated LPA-induced RhoA activation, whereas silencing of MAGI-3 by siRNA resulted in a small but statistically significant decrease in RhoA activation. These results demonstrate that MAGI-3 interacts directly with LPA_2 and regulates the ability of LPA_2 to activate Erk and RhoA.

Keywords: Lysophosphatidic acids; PDZ; MAGI-3; Receptor

1. Introduction

Lysophosphatidic acids (LPA) exert growth factor-like effects such as proliferation, apoptosis, contraction, migration, and aggregation of platelets [1–4]. Signaling by LPA is primarily mediated through LPA_1, LPA_2 and LPA_3, which are members of a family of G protein-coupled receptors (GPCRs). LPA_1, LPA_2, and LPA_3 are highly homologous with more than 50% identity [5–7]. Recently, an orphan receptor P2Y9/GPR23 has been identified as the fourth LPA receptor [8]. P2Y9/GPR23, despite sharing only 20–24% amino acid identity with the other LPA receptors, mediates adenylate cyclase stimulation and intracellular Ca^{2+} mobilization in response to LPA. All the LPA receptors can couple to three distinct families of heterotrimeric GTP binding proteins, including $G_{q/11}$, $G_{i/0}$, and $G_{12/13}$ [3,9]. The best known pathway triggered by LPA is the activation of phospholipase C (PLC) with subsequent phosphatidylinositol-(4,5)-biphosphate hydrolysis and Ca^{2+} mobilization. This pathway involves a pertussis toxin (PTX)-insensitive $G_{q/11}$-mediated mechanism as well as a PTX-sensitive $G_{i/o}$-mediated mechanism depending on cell types. This classical $G\alpha_q$-PLC-Ca^{2+} cascade can also mediate mitogen-activated protein kinase (MAPK) activation. We have previously shown that LPA-induced activation of extracellular signal regulated kinase 1 and 2 (Erk1/2) in human colon cancer cells was completely blocked by the PLCβ inhibitor, U73122 [10]. In contrast, the activation of the PI3K–Akt pathway was PTX-sensitive, suggesting a G_i-mediated mechanism is involved. It is also evident that LPA receptors couple to $G_{12/13}$ to activate the

* Corresponding author. Department of Medicine, Emory University School of Medicine, Atlanta, GA 30322, USA. Tel.: +1 404 712 2865; fax: +1 404 727 5767.
E-mail address: ccyun@emory.edu (C.C. Yun).

0898-6568/$ - see front matter © 2006 Elsevier Inc. All rights reserved.
doi:10.1016/j.cellsig.2006.06.008

small GTPase RhoA that mediates the remodeling of the actin cytoskeleton [11,12]. Recent studies have shown that the activation of RhoA is mediated by RhoGEFs that serve as effectors of activated $G_{12/13}$ and a molecular bridge between the G-proteins and RhoA [11].

The formation of protein complexes is the basis for efficient propagation in many cellular signaling processes. In this regard, the PDZ domain has emerged as a major mediator of protein sequestration in the plasma membrane. The PDZ domain was identified as a common element present in *P*SD-95, the *D*rosophila disc-large tumor suppressor protein DlgA and the tight-junction protein *Z*O-1. The PDZ domain is made up of ~90 amino acid residues that preferentially bind to distinct peptide sequences located at the carboxyl-terminus (CT) of interacting proteins [13,14]. Class I PDZ domains preferentially bind to the CT motif-S/T-x-Φ, where Φ represents a hydrophobic amino acid [15]. Many receptors possess Class I PDZ binding motifs at their carboxyl-termini. These include the β_2-adrenergic receptor (β_2-AR), $P2Y_1$ receptor, and *N*-methyl-D-aspartate (NMDA) receptors, to name a few [16–18]. PDZ interaction can regulate receptor-mediated signaling, the recycling and trafficking of receptors, and assembly of receptors with other proteins at the plasma membrane.

LPA_1 and LPA_2 possess Class I carboxyl-terminal motifs that allow interaction with PDZ domain-containing proteins. We and others have reported that LPA_2, but not LPA_1, binds specifically to the Na^+/H^+ exchanger regulatory factor 2 (NHERF2; also known as E3KARP) [10,19]. NHERF2 links LPA_2 to PLC-β3 and, hence, affects the activation of downstream targets, such as Erk and cyclooxygenase-2 [19]. In addition, it has been shown that PTX-sensitive activation of Akt is drastically down-regulated by knockdown of NHERF2 expression [10]. In contrast to the LPA_2-specific association with NHERF2, both LPA_1 and LPA_2 bind to PDZ domain-containing RhoGEFs and regulate LPA-induced RhoA activation via $G_{12/13}$ [11,20]. However, because of the abundance of PDZ domains (~440 PDZ domains in the human genome [15]), it is likely that there are additional PDZ scaffolds that can associate with LPA_2 and LPA_1, and thus there is a clear physiological need to identify these PDZ scaffolds. In this study, we have used a newly developed PDZ proteomic array to identify additional PDZ proteins that interact with LPA_2 [17,21]. We identified several novel interactions, and examined in detail the association between LPA_2 and the membrane-associated guanylate kinase-like protein with an inverted domain structure-3 (MAGI-3).

2. Materials and methods

2.1. Chemicals and plasmid constructs

1-Oleoyl-2-Hydroxy-*sn*-Glycero-3-Phosphatidic acid was obtained from Avanti Polar Lipids and prepared in PBS containing 0.1% BSA (v/v). The LPA_2-selective agonist, fatty alcohol phosphate (FAP-12) [22], was purchased from BIOMOL. Monoclonal anti-V5 was from Covance, and polyclonal anti-MAGI-3 antibody was obtained from BD Biosciences. Anti-LPA_2 against the N-terminus was purchased from Exalpha Biologicals, Inc. All other antibodies were purchased from Cell Signaling.

The carboxyl-terminal (CT) 56, 44, and 43 amino acids of LPA_1, LPA_2, and LPA_3, respectively, were cloned into pGEX-4T to generate GST fusion proteins. Full-length MAGI-3 in pcDNA3.1/V5–His was kindly provided by Rich Laura (Genetech). The individual PDZ domains of MAGI-3 (PDZ1: 429–579, PDZ2: 597–742, PDZ3: 745–873, PDZ4: 874–1022, PDZ5: 1040–1151) were cloned into pET30A as previously described [17].

2.2. PDZ array and in vitro overlay assay

PDZ domains expressed as His- and S-tagged fusion proteins spotted on gridded nylon membranes were previously described [17,21]. The membranes were blocked in blot buffer (10 mM Hepes, pH 7.4, 50 mM NaCl, 2% dry milk, 0.1% Tween 20) for 30 min at room temperature, then overlaid with 100 nM GST-LPA_2 fusion proteins in blot buffer for 1 h at room temperature. The membranes were washed three times in blot buffer, and incubated with HRP-conjugated anti-GST antibody to detect GST fusion protein overlaid on His-PDZ fusion proteins using the ECL kit (Pierce Biotech).

The carboxyl-terminal (CT) 56, 44, and 43 amino acids of LPA_1, LPA_2, and LPA_3, respectively, were cloned into pGEX-4T to generate GST fusion proteins. His- and S-tagged PDZ domains of MAGI-3 were run on 15% SDS-PAGE gels, blotted and overlaid with 50 nM GST-LPA_1, GST-LPA_2, GST-LPA_3, or GST in blot buffer for overnight at 4 °C. The blots were washed three times in the same buffer and incubated for 1 h at room temperature with anti-GST antibody, followed by horseradish peroxidase conjugated secondary antibody to detect GST fusion protein overlaid on His-PDZ fusion proteins.

The DSTL motif at the CT of GST-LPA_2 was sequentially mutated to Ala by PCR. GST fusion proteins were expressed, separated by SDS-PAGE, and transferred onto nylon membranes. The membrane was blocked and overlaid with 50 nM His- and S-tagged PDZ5 of MAGI-3 as described earlier. The membranes were washed three times in blot buffer, and incubated with HRP-conjugated S protein (Novagen) to detect the PDZ5 protein overlaid on GST fusion proteins.

2.3. Cell culture, transfection and RNA preparation

SW480 cells obtained from the American Tissue Culture Collection were grown in RPMI-1640 supplemented with 10% FBS, 100 μg/ml streptomycin and 100 U/ml penicillin at 37 °C in 95% air/5% CO_2 atmosphere as previously described [23]. Transfection was performed using Lipofectamine2000 as recommended by the manufacturer (Invitrogen). When appropriate, cells were selected with 800 μg/ml G418.

siRNA targeting human MAGI-3 was purchased from Invitrogen. SW480 cells seeded at 50% confluence on 60 mm culture plates were transfected with 20 nM siRNA using Lipofectamine2000. As control, a scrambled 21 nt RNA duplex also purchased from Invitrogen was used. Twenty-four hours after transfection, cells were serum deprived overnight and next morning treated with LPA or carrier. The efficacy of gene silencing was determined by Western immunoblot using an anti-MAGI-3 antibody.

Total RNA was prepared from cells by using TRIzol (Invitrogen), followed by reverse transcription to generate cDNA using the First Strand Synthesis kit (Invitrogen). The primer pairs specific for LPA_{1-3} and β-actin, and the conditions for semi-quantitative amplification have been previously described [10].

2.4. Western immunoblot and in vivo interaction

Cells were rinsed three times with ice-cold PBS buffer, and lysed by sonication in lysis buffer composed of 50 mM Tris–Cl, pH 7.4, 150 mM NaCl, 1 mM EDTA, 0.1 mM PMSF, 1 mM Na orthovanadate, 10 mM Na fluoride, 10 mM Na pyrophosphate, 25 mM β-glycerophosphate, 1% Triton X-100, and protease inhibitors (one complete Mini EDTA-free protease inhibitor cocktail tablet per 10 mL; Roche Applied Science). The lysates were cleared by centrifugation at 14,000 *g* at 4 °C for 10 min. Protein concentration was determined by the Bicinchoninic Acid assay (Sigma). The equal amount of lysate in 2× Laemmli sample buffer was resolved by 6% SDS-PAGE, and Western immunoblot analysis was performed as previously described [10]. To determine the activation of Erk, serum starved cells were activated with 10 μM LPA and lysates were prepared as described above. The levels of activated Erk were determined using an anti-phospho-Erk antibody (1:1000; Cell Signaling). The filters were stripped and reprobed with an anti-Erk antibody to analyze total protein levels. The levels of phosphor-Erk were normalized to total Erk by densitometric analysis. Activation of Akt was determined by a similar approach.

SW480/MAGI-3 or SW480/pcDNA cells were treated with 10 μM LPA or a carrier for 10 min cells were washed twice in ice-cold PBS and lysed in lysis buffer. Lysates were cleared by centrifugation and one milligram of lysate was incubated with 60 μl Ni-NTA beads (1:1 mix) (Qiagen) for 1 h at 4 °C with constant head-over-tail rotation. The resins were washed three times with lysis buffer and the bound proteins were eluted from the resins by boiling for 5 min in 2× Laemmli sample buffer. Western blot was performed as described above.

Densitometric analyses were performed on the Typhoon phosphoimager (Amersham) using the Image Quant program. Statistical significance was assessed by one-way ANOVA using Origin software. Data are presented as the means±standard deviation (SD).

2.5. RhoA activation assay

Activation of RhoA was determined by a modified method described by Ren and Schwartz [24]. Cells were seeded on 60-mm culture dishes. When gene silencing by siRNA was needed, cells were prepared and transfected as described earlier. After serum starvation for 24 h, cells were activated with LPA and lysed in ice-cold lysis/binding buffer (25 mM Tris–HCl, pH 7.5, 150 mM NaCl, 5 mM $MgCl_2$, 1% NP-40, 1 mM DTT, 10% glycerol, and protease inhibitors). Three hundred micrograms of lysate was incubated for 1 h with glutathione-sepharose beads (Amersham) coupled with the Rho-binding domain of rhotekin (GST-RBD). The construct to express GST-RBD was kindly provided by Dr. Martin Schwarts (Univ. of Va). Beads were washed three times with lysis/binding buffer, and the bound RhoA proteins were eluted with Laemmli sample buffer and subjected to Western blot using an anti-RhoA antibody.

3. Results

3.1. Identification of PDZ proteins interacting with LPA_2

Previous studies have shown that LPA_2 interacts with two PDZ proteins, NHERF2 and PDZ-rhoGEF [10,19,20]. To further identify PDZ domains that interact with LPA_2, we screened a PDZ domain proteomic array that contains 96 distinct PDZ domains expressed and purified as His-tagged proteins [17]. This blot was overlaid with GST fusion proteins corresponding to LPA_2 CT. Fig. 1 shows that GST-LPA_2 interacted with several of the PDZ domains on the array. These included MAGI-2/PDZ5, NHERF1/PDZ1, NHERF2/PDZ2, MAGI-3/PDZ5, and neurabin [25,26]. The strongest signals were observed with NHERF2/PDZ2 and MAGI-2/PDZ5. The binding of the CT of LPA_2 to NHERF2/PDZ2 has previously been demonstrated [10,19]. As

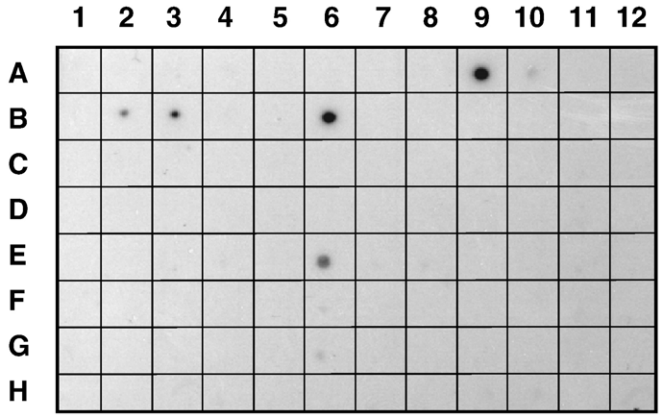

	1	2	3	4	5	6	7	8	9	10	11	12
A	MAGI-1 PDZ1	MAG-1 PDZ2	MAGI-1 PDZ3	MAGI-1 PDZ4+5	MAGI-2 PDZ1	MAGI-2 PDZ2	MAGI-2 PDZ3	MAGI-2 PDZ4	MAGI-2 PDZ5	MAGI-3 PDZ1	Enigma PDZ	MAGI-3 PDZ3
B	MAGI-3 PDZ4	MAGI-3 PDZ5	NHERF1 PDZI	NHERF1 PDZ2I	NHERF2 PDZ1	NHERF2 PDZ2	PSD95 PDZ1+2	PSD95 PDZ3	CNRasGEF1 PDZ	CAL PDZ	nNOS PDZ	INADL PDZ5
C	INADL PDZ6	PTPN3 PDZ	SAP97 PDZ1+2	SAP97 PDZ3	SAP102 PDZ1+2	SAP102 PDZ3	Chap110 PDZ1+2	Chap110 PDZ3	E6TP1 PDZ	ERBIN PDZ	Z01 PDZ1	Z01 PDZ2
D	Z01 PDZ3	Z02 PDZ1	Z02 PDZ2	Z02 PDZ3	Z03 PDZ1	Z03 PDZ2	Z03 PDZ3	C2PA PDZ	GIPC PDZ	MALS-1 PDZ	PTPN4 PDZ	MALS-3 PDZ
E	Densin180 PDZ	Rophilin1 PDZ	Rhophilin2 PDZ	Harmonin PDZ1	Harmonin PDZ2	Neurabin PDZ	Spinophilin PDZ	α1 syntrophin PDZ	β1 syntrophin PDZ	β2 syntrophin PDZ	γ1 syntrophin PDZ	γ2 syntrophin PDZ
F	PAPIN-1 PDZ	MUPPI PDZ1	PAR 3 PDZ1	MUPPI PDZ6	MUPPI PDZ7	MUPPI PDZ8	MUPPI PDZ10	MUPPI PDZ12	MUPPI PDZ13	PTPN13 PDZ1	PAR3 PDZ2	PTPN13 PDZ3
G	PTPN13 PDZ4+5	PDZK1 PDZ1	PDZK1 PDZ2	PDZK1 PDZ3	PDZK1 PDZ4	PDZK2 PDZ1	PDZK2 PDZ2	PDZK2 PDZ3	PDZK2 PDZ4	LNX1 PDZ1	LNX1 PDZ2	LNX1 PDZ3
H	LNX1 PDZ4	LNX2 PDZ1	LNX2 PDZ2	PAR2 PDZ3	LNX2 PDZ4	LARG PDZ	MAST205 PDZ	RA-GEF PDZ	Rho-GEF PDZ	Tamalin PDZ	Shank PDZ	ALP PDZ

Fig. 1. A proteomic analysis to identify LPA_2 binding PDZ domains. The CT of LPA_2 fused to GST was overlaid onto a proteomic array containing 96 distinct Class I PDZ domains. GST-LPA_2 showed specific binding to several PDZ domains, including MAGI-2/PDZ5 (A9), MAGI-3/PDZ5 (B2), NHERF1/PDZ1 (B3), NHERF2/PDZ2 (B6), and neurabin (E6). Representative data from 3 separate experiments are shown. The list of the PDZ domains spotted on the membrane is shown on the bottom. A detailed description of the PDZ domains has previously been published [21].

previously been shown [17], GST itself did not bind to the PDZ domains. MAGI-3 is widely expressed in multiple tissues including brain, heart, and colon, whereas MAGI-2 and neurabin are preferentially expressed in the brain [27–29]. Because of our interest in the role of LPA_2 in gastrointestinal physiology, we characterized the interaction between LPA_2 and MAGI-3 in further detail.

3.2. Specificity of the LPA_2 interaction with MAGI-3/PDZ3

LPA_1 and LPA_2 have CT motifs of -HSVV and -DSTL, respectively, that are likely to interact with PDZ domains. In contrast, LPA_3 has the CT motif -KSTS. To confirm that the specificity of the interaction with MAGI-3, we performed in vitro overlay assays. Individual PDZ domain of MAGI-3 expressed as His- and S-tagged fusion proteins were overlaid with GST-LPA_1, GST-LPA_2, GST-LPA_3, or GST as shown in Fig. 2A. Overlay studies revealed that GST-LPA_2 robustly bound to PDZ5 of MAGI-3. In contrast, GST-LPA_1, GST-LPA_3 or GST showed no interaction with any of the PDZ domains of MAGI-3. Please note that the bands labeled with asterisks on the blots overlaid with LPA_1 and LPA_3 are not the PDZ4 domain, but a contaminating *E. coli* protein that was present in the preparation of MAGI-3/PDZ4. For an unknown reason, GST-LPA_1 and GST-LPA_3, or proteolytic byproducts of the GST fusion proteins repeatedly bound to this product, which migrated as a smaller molecular mass (asterisk) than that of MAGI-3/PDZ4 (arrowhead).

The above results showed that LPA_1, despite having a Class I PDZ-binding motif, is unable to bind to MAGI-3. To further analyze the specificity of the interaction between LPA_2 and MAGI-3/PDZ5, the amino acids comprising the DSTL motif of LPA_2 were sequentially mutated to Ala. Fig. 2B shows a robust association between MAGI-3/PDZ5 and GST-DSTL, consistent with the data shown in Fig. 1. However, this association between LPA_2 and MAGI-3 was completely abolished by the replacement of the terminal Leu, suggesting that the Leu is essential. Mutation of Asp at −3 or Ser at −2 did not completely abolish, but drastically inhibited the binding of MAGI-3/PDZ5, suggesting that these amino acid residues are important, but not obligatory. In contrast, the replacement at the −1 did not affect the binding to MAGI-3/PDZ3.

To corroborate the results of the in vitro studies on LPA_2 and MAGI-3, we next tested the association between MAGI-3 and LPA_2 in living cells. SW480 cells transfected with V5/His-MAGI-3 or pcDNA3.1/V5–His were treated with 10 μM LPA or carrier for 10 min. Exogenous V5/His-MAGI-3 was affinity-purified using Ni-NTA resins and the presence of co-purified LPA_2 was determined by Western blot (Fig. 2C). The results showed that LPA_2 co-purified from lysates of SW480 cells transfected with MAGI-3, but not pcDNA. In addition, treatment with LPA did not affect the amount of LPA_2 co-purified, suggesting that the LPA_2–MAGI-3 association was not regulated by LPA but appeared to occur constitutively.

3.3. MAGI-3 potentiates LPA-induced activation of Erk, but not Akt

We have previously shown that SW480 and several other human colon cancer cell lines predominantly express LPA_2

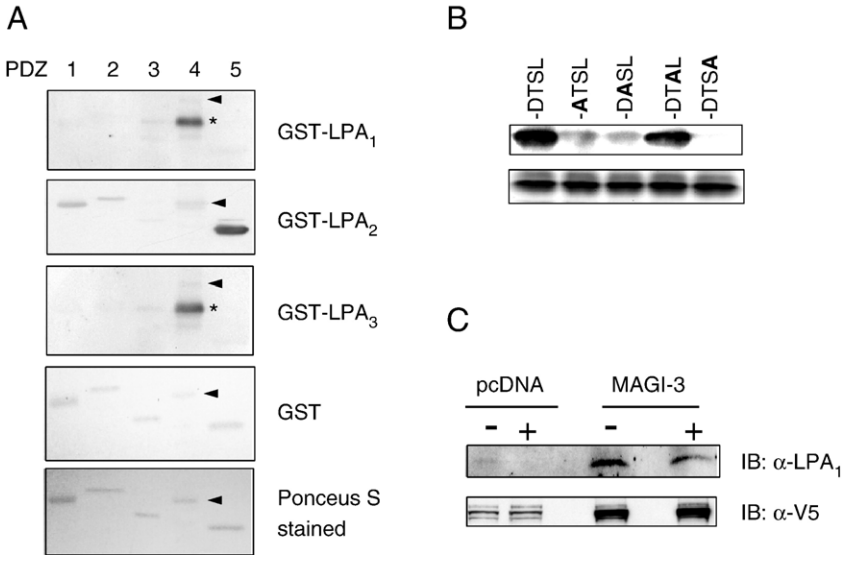

Fig. 2. LPA_2 specifically binds to MAGI-3. A. GST fusion constructs of LPA_{1-3} CT were overlaid onto membranes containing the individual PDZ domains of MAGI-3. LPA_2, but not LPA_1 or LPA_3, bound to the PDZ5 domain of MAGI-3. The bottom panel shows a representative Ponceau-S stained transfer membrane containing purified PDZ domains. Asterisk (*) indicates a contaminating *E. coli* protein. Arrow heads point to the location of PDZ4. B. Structural determinants of the LPA_2–MAGI-3 interaction. The last four amino acids (DTSL) of LPA_2 CT were sequentially mutated to Ala. Substituted Ala residues are highlighted in bold. Wild-type and mutated LPA_2 CT were expressed as GST fusion proteins (3 μg), loaded onto SDS-PAGE gels, transferred, and overlaid with His- and S-tagged PDZ5 of MAGI-3. All data are representative of four independent experiments. The bottom panel shows a representative Coomasie-stained gel showing equal loading of the GST fusion proteins. C. Co-affinity purification of MAGI-3 and LPA_2 from SW480 cells. SW480 transfected with V5/His-MAGI-3 or pcDNA3.1–V5/His were treated with 10 μM LPA or carrier for 10 min. V5/His-MAGI-3 was affinity purified and the presence of co-purified LPA_2 was detected by Western blot. Bottom panel shows Western blot using an anti-V5 antibody indicating the presence of affinity-purified V5/His-MAGI-3 in SW480/MAGI-3 cells. Representative data from four independent experiments are shown.

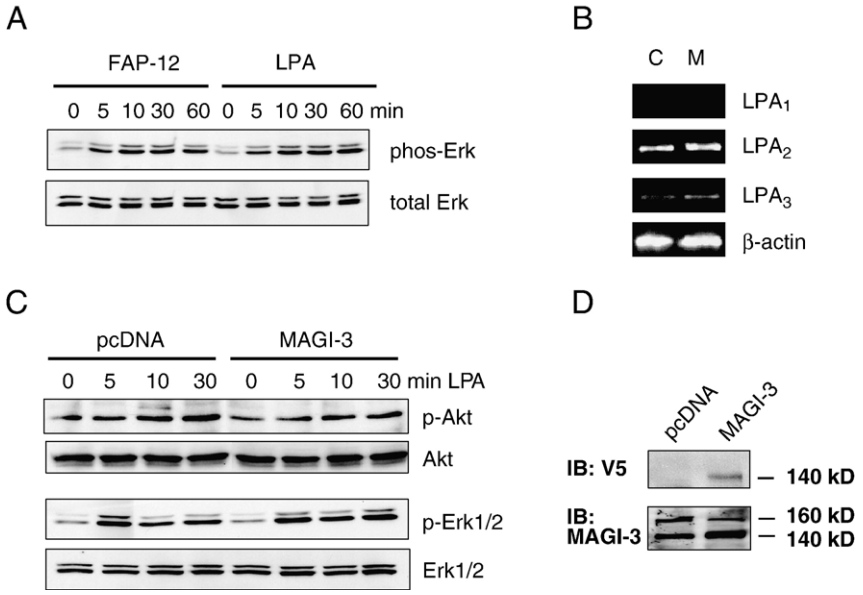

Fig. 3. LPA-induced activation of Akt and Erk. A. SW480 cells were activated by 10 μM LPA or 10 μM FAP-12. Activation of Erk was determined by Western blot using an anti-phospho-Erk antibody as described under Materials and methods. B. RT-PCR was performed on RNA prepared from SW480 cells stably transfected with pcDNA3.1/V5–His (C) or V5/His-MAGI-3 (M). C. SW480/pcDNA and SW480/MAGI-3 cells were treated with LPA, and the amounts of activated Akt and Erk were determined using anti-phospho-Akt and anti-phospho-Erk antibodies, respectively. Anti-Akt or anti-Erk antibodies were used to determine total Akt and Erk, respectively. Results are representative of five independent experiments. D. The expression levels of exogenous V5/His-MAGI-3 were determined by Western blot using an anti-V5 antibody. An anti-MAGI-3 antibody was used to compare total MAGI-3 proteins in V5/His-MAGI-3 and control transfected cells.

(Fig. 3B) [10]. To confirm that LPA_2 is the major LPA receptor in SW480 cells, we stimulated the cells with LPA or FAP-12. FAP-12 is a specific agonist of LPA_2, yet a selective antagonist of LPA_3 and LPA_1 [22]. As shown in Fig. 3A, the magnitude and time-course of Erk activation by LPA and FAP-12 were identical, suggesting that LPA-induced signaling is primarily elicited by LPA_2. To address a potential role of MAGI-3 in LPA-induced signaling in colon cancer cells, we used SW480 cells stably transfected with V5/His-MAGI-3 or pcDNA as control. Overexpression of MAGI-3 did not alter the expression levels of LPA receptors (Fig. 3B). Induction of LPA_2 activates several downstream targets, including Erk and Akt. However, overexpression of MAGI-3 did not affect the amplitude or time-course of Akt activation (Fig. 3C). Similarly, LPA-mediated Erk

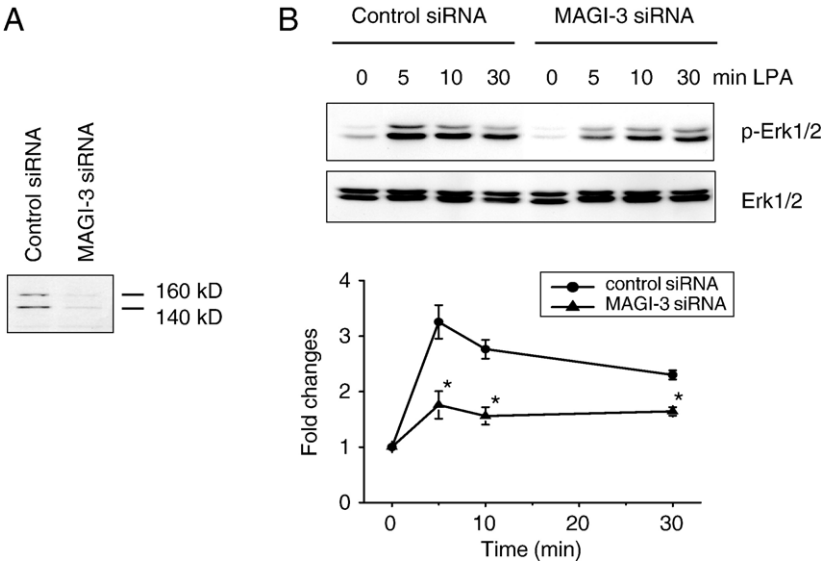

Fig. 4. Knockdown of MAGI-3 significantly affects LPA-induced activation of Erk. A. The expression level of MAGI-3 in MAGI-3 siRNA treated cells was decreased to 18±4% of control siRNA treated cells. B. Time-course of LPA-induced activation of Erk in MAGI-3 siRNA and control siRNA treated cells were determined as described under Materials and methods. Representative data from four independent experiments are shown. The amount of phospho-Erk was quantified and was presented as fold-changes over the amount of phospho-Erk in untreated cells. The bars and error bars represent means±SD. *indicates $p<0.01$ relative to the control transfected cells.

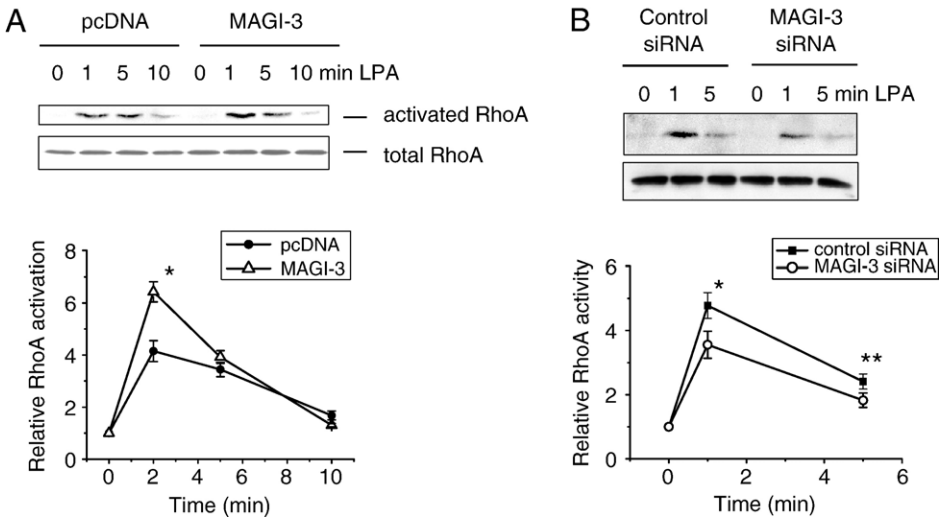

Fig. 5. Effects of MAGI-3 on LPA-induced RhoA activation. A. SW480 cells transfected with V5/His-MAGI-3 or pcDNA were treated with LPA, and the lysates (300 μg) were incubated with GST-rhotekin RhoA binding domain (GST-RBD). The bound activated RhoA was resolved by SDS-PAGE, transferred, and blotted using an anti-RhoA antibody to determine the extent of RhoA activation. Total RhoA was determined using lysates. Data are means ± SD of four independent experiments. * indicates $p < 0.01$ compared with control siRNA treated cells. B. The activation of RhoA in cells treated with MAGI-3 siRNA or control siRNA was determined. *, ** indicate $p < 0.01$ and $p < 0.10$, respectively, compared with control transfected cells.

activation was not altered significantly by overexpression of MAGI-3. We contemplated that the lack of effect might be due to a limited increase in the total amount of MAGI-3 protein over the endogenous level. MAGI-3 protein migrates as a 140 kDa band with a minor band at 170 kDa, and V5-tagged MAGI-3 migrated at 140 kDa (Fig. 3D) [30]. A comparison of total MAGI-3 protein in the transfected cells using an anti-MAGI-3 antibody revealed that the heterologous expression of MAGI-3 only modestly increased (~25%) the total amount of MAGI-3 (Fig. 3D). To circumvent this limitation, we employed siRNA to silence MAGI-3 expression in SW480 cells. Transient transfection of SW480 cells with siRNA targeting MAGI-3 resulted in an approximately 80% decrease in the amount MAGI-3 proteins, as determined by Western blot (Fig. 4A). Subsequent determination of Erk activation (Fig. 4B) revealed that knockdown of MAGI-3 significantly decreased LPA-induced activation of Erk. In contrast, knockdown of MAGI-3 had no effect on Akt activation (data not shown).

3.4. MAGI-3 facilitates LPA-induced RhoA activation

LPA receptors couple with $G\alpha_{12/13}$ to activate the small GTPase RhoA [31]. To examine whether MAGI-3 regulates RhoA activation by LPA, we determined RhoA activation by using the GST-Rho binding domain of Rhotekin (GST-RBD) in SW480/pcDNA and SW480/MAGI-3 cells. LPA rapidly activated RhoA in control transfected cells, reaching maximum activity at 1–2 min. A similar activation of RhoA was observed in MAGI-3 overexpressing cells (Fig. 5A). Quantification showed that the activation of RhoA in SW480/MAGI-3 cells was more robust (31%) compared with control transfected cells. Conversely, knockdown of MAGI-3 decreased LPA-induced activation of RhoA (15%) compared with control siRNA treated cells (Fig. 5B). However, the extent of the reduction in RhoA activation by MAGI-3 knockdown was smaller compared to the effect on Erk activation by overexpression.

4. Discussion

Lysophosphatidic acid (LPA) is a mediator of multiple cellular responses. LPA mediates its effects predominantly through the G protein-couple receptors, LPA_1, LPA_2, and LPA_3. Recent studies have shown that scaffold proteins, such as NHERF2 and TRIP6, play a pivotal role in LPA-induced signaling [10,19,32]. LPA_2 has a canonical PDZ binding motif, -DSTL, at its carboxyl-terminus. Thus far, three PDZ-containing proteins, NHERF2, PDZ-RhoGEF, and leukemia-associated RhoGEF (LARG), have been shown to bind to the carboxyl-terminus of LPA_2 [10,11,19,20]. These proteins have been identified by testing the associations with LPA_2 under an assumption that LPA_2 may interact with their PDZ domains. To further identify additional PDZ proteins that may interact with LPA_2, we employed a proteomic approach. The PDZ proteomic arrays have previously been used by us in the identification of PDZ proteins interacting with GPCRs such as $P2Y_1$ and β-ARs [17,21]. Using the PDZ arrays containing 96 individual PDZ domains, we found that LPA_2 binds to several PDZ scaffolds, including NHERF2 and MAGI-3. This is a sensitive in vitro assay as evident by the binding of GST-LPA_2 to NHERF1 in the proteomic array, although we and others have previously shown that this association does not occur in vivo [10,19]. On the other hand, we were not able to observe the binding of the GST-LPA_2 to the PDZ domains of RhoGEF or LARG under the experimental conditions. Thus, the list of PDZ domains identified here is certainly not exhaustive and there may be additional PDZ proteins that can associate with LPA_2.

Our data reported here demonstrated that LPA_2 specifically interacted with MAGI-3. LPA_2 preferentially bound to the fifth PDZ domain of MAGI-3 as demonstrated by both the proteomic

arrays and in vitro overlay assays. We also showed that LPA_1, despite having a Class I PDZ domain interacting sequence, -SVV, was not able to bind to MAGI-3. A similar preference for LPA_2 over LPA_1 has been observed with NHERF2. In contrast, PDZ-RhoGEF and LARG bind to both LPA_2 and LPA_1 with similar efficacy [20]. Our mutational analysis of LPA_2 carboxyl-terminus showed that, in addition to the terminal Leu, there was a strong preference for Asp at the −3 position of LPA_2, which is absent in LPA_1. Studies have previously shown that the presence of an acidic amino acid at −3 can greatly influence the PDZ binding characteristics, and NMDA receptors, the only other protein known to bind to MAGI-3/PDZ5, also possess an acidic amino acid at the −3 position [16,17,21,27].

Among the PDZ domains identified, we have chosen to study the association between LPA_2 and MAGI-3, since MAGI-3 is ubiquitously expressed in all tissues, including the gastrointestinal tract [27,28]. In human colonic epithelial Caco-2 cells, MAGI-3 has been found at the apical membrane and the nucleus as well as at tight junctions [30]. In contrast, the expression of MAGI-2 is largely limited to the brain although localized expression in other types of tissue has been reported [33]. MAGI-3 contains multiple protein interacting domains, including 5 PDZ domains, 2 WW domains, and a guanylate kinase domain [27]. Through these protein-interacting domains, MAGI-3 is able to interact with a number of proteins, including frizzled, PTEN/MMAC, transforming growth factor-α, and receptor tyrosine phosphatase-β [27,30,34,35]. Recently, MAGI-3 has been shown to associate with β_1-AR and impair the receptor's G_i-mediated signaling [21]. In colon cancer cells, we have previously demonstrated that LPA_2 activates Akt via a PTX-sensitive pathway [10]. In the current study, overexpression or knockdown of MAGI-3 did not affect the G_i-mediated Akt activation, suggesting that MAGI-3 does not always impact the G_i-mediated pathway and that the effect of MAGI-3 on the G_i-mediated signaling is likely to be receptor dependent. Unlike the previous studies where overexpression or knockdown of PDZ-proteins results in a drastic change in signaling, knockdown of MAGI-3 did not completely abrogated LPA-induced signaling. We reason that the residual signaling must be facilitated via either the remaining MAGI-3 (20% or less) in SW480/MAGI-3 cells or other PDZ proteins expressed in these cells. NHERF2, which also interacts with LPA_2, is expressed in SW480 as well as other colon cancer cells. Previous studies have shown that NHERF2 also facilitates the activation of Erk by LPA_2, and knockdown of NHERF2 resulted in partial attenuation of Erk activation, a result similar to that by MAGI-3 knockdown.

The present study shows that overexpression of MAGI-3 did not exert any measurable effect on the activation of Erk, whereas there was a clear increase in RhoA activation. Although we do not know the reasons behind these discriminating effects by MAGI-3, one possibility is that MAGI-3 facilitates activation of Erk and RhoA with differential efficiency. The results suggest that LPA-induced Erk activation is efficiently mediated, probably to its full capacity, through the interaction with endogenous MAGI-3 such that exogenously expressed MAGI-3 failed to influence the signal transduction. Therefore, knockdown of MAGI-3, but not overexpression, was able to alter the magnitude of LPA-induced Erk activation. We found that the effect of MAGI-3 on RhoA differed from its effect on Erk. The positive effect on RhoA by overexpression implies that endogenous MAGI-3 has a limited capacity to regulate RhoA in response to LPA. Hence, overexpression of MAGI-3 led to an increase in RhoA activation over the basal activation level. In contrast, the limited RhoA activation via MAGI-3 resulted in a modest effect by knockdown of MAGI-3.

It is well established that G proteins of the G_{12}-family, G_{12} and G_{13}, can couple GPCRs to activate RhoA. It is generally accepted that LPA-induced RhoA activation is mediated by $G_{12/13}$. Studies have shown a role of Rho-specific exchange factors, PDZ-RhoGEF and LARG, in linking $G_{12/13}$ and RhoA [11,20,36]. However, an unidentified protein-tyrosine kinase has been implicated in RhoA activation, suggesting that the presence of $G_{12/13}$ and a RhoGEF is not sufficient for efficient RhoA activation [31]. In addition, it has been shown using $G_{12/13}$-deficient mouse embryonic fibroblasts that G_q-mediated signaling can contribute to RhoA activation [12]. A recent study has shown that RhoA activation can occur via distinct pathways involving $G\alpha_{12/13}$ or $G\alpha_q$ such that the expression of activated $G\alpha_q$ in HEK293T cells led to a robust activation of RhoA in a $G\alpha_{13}$-independent mechanism [37]. Although the mechanism of $G\alpha_q$-mediated RhoA activation is not clear, it seems that $G\alpha_q$ mediates RhoA activation independent of PLCβ or elevation of intracellular Ca^{2+} [12]. We speculate that MAGI-3 might be able to interact with $G\alpha_q$ based on a previous report that the constitutively activated $G\alpha_q$ mutant can bind to a PDZ domain [38]. Hence, MAGI-3 may enhance the coupling of $G\alpha_q$ to LPA_2, facilitating the $G\alpha_q$-dependent activation of Erk and RhoA. On the other hand, it is possible that signaling intermediates necessary for Erk or RhoA activation bind at distinct sites within MAGI-3 such that LPA_2 activates Erk and RhoA independently. MAGI-3 possesses multiple protein-interacting domains and thus appears capable of mediating concomitant interactions with more than one protein.

This study demonstrates that MAGI-3 is coupled to LPA_2 receptor. The interaction with MAGI-3 is specific to LPA_2, but not to LPA_1 or LPA_3. The coupling of MAGI-3 facilitates LPA_2-mediated activation of Erk and RhoA. In light of recent studies showing overexpression of LPA_2 in several types of cancers and the roles of LPA in activation of oncogenic signal pathways [10,39–41], the current findings suggest that MAGI-3 may potentially enhance cell survival and gene transcription via the activation of Erk and RhoA.

Acknowledgement

This work was supported by the National Institutes of Health (R.A.H. and C.C.Y.), the W.M. Keck Foundation (R.A.H.), the Emory University Research Committee (C.C.Y.), and the Emory Epithelial Pathobiology Research Development Center (C.C.Y.). We would like to thank Dr. Martin Schwarts for GST-RBD and Amenda Castleberry for the technical assistance in PDZ proteomic screen.

References

[1] G. Tigyi, A.L. Parrill, Prog. Lipid Res. 42 (2003) 498.
[2] X. Ye, I. Ishii, M.A. Kingsbury, J. Chun, Biochim. Biophys. Acta 1585 (2002) 108.
[3] E.J. Goetzl, S. An, FASEB J. 12 (1998) 1589.
[4] O. Kranenburg, W.H. Moolenaar, Oncogene 20 (2001) 1540.
[5] S. An, M.A. Dickens, T. Bleu, O.G. Hallmark, EJ. Goetzl, Biochem. Biophys. Res. Comm. 231 (1997) 619.
[6] S. An, T. Bleu, O.G. Hallmark, E.J. Goetzl, J. Biol. Chem. 273 (1998) 7906.
[7] J. Aoki, K. Bandoh, K. Inoue, Ann. N. Y. Acad. Sci. 905 (2000) 263.
[8] K. Noguchi, S. Ishii, T. Shimizu, J. Biol. Chem. 278 (2003) 25600.
[9] W.H. Moolenaar, Exp. Cell. Res. 253 (1999) 230.
[10] C.C. Yun, H. Sun, D. Wang, R. Rusovici, A. Castleberry, R.A. Hall, H. Shim, Am. J. Physiol. 289 (2005) C2.
[11] Q. Wang, M. Liu, T. Kozasa, J.D. Rothstein, P.C. Sternweis, R.R. Neubig, J. Biol. Chem. 279 (2004) 28831.
[12] S. Vogt, R. Grosse, G. Schultz, S. Offermanns, J. Biol. Chem. 278 (2003) 28743.
[13] A.S. Fanning, J.M. Anderson, J. Clin. Invest. 103 (1999) 767.
[14] Z. Songyang, A.S. Fanning, C. Fu, J. Xu, S.M. Marfatia, A.H. Chishti, A. Crompton, A.C. Chan, J.M. Anderson, LC. Cantley, Science 275 (1997) 73.
[15] A.Y. Hung, M. Sheng, J. Biol. Chem. 277 (2002) 5699.
[16] R.A. Hall, L.S. Ostedgaard, R.T. Premont, J.T. Blitzer, N. Rahman, M.J. Welsh, R.J. Lefkowitz, Proc. Natl. Acad. Sci. U. S. A. 95 (1998) 8496.
[17] S.R. Fam, M. Paquet, A.M. Castleberry, H. Oller, C.J. Lee, S.F. Traynelis, Y. Smith, C.C. Yun, R.A. Hall, Proc. Natl. Acad. Sci. U. S. A. 102 (2005) 8042.
[18] H.J. Chung, Y.H. Huang, L.F. Lau, R.L. Huganir, J. Neurosci. 24 (2004) 10248.
[19] Y.S. Oh, N.W. Jo, J.W. Choi, H.S. Kim, S.W. Seo, K.O. Kang, J.I. Hwang, K. Heo, S.H. Kim, Y.H. Kim, I.H. Kim, J.H. Kim, Y. Banno, S.H. Ryu, P.G. Suh, Mol. Cell. Biol. 24 (2004) 5069.
[20] T. Yamada, Y. Ohoka, M. Kogo, S. Inagaki, J. Biol. Chem. 280 (2005) 19358.
[21] J. He, M. Bellini, H. Inuzuka, J. Xu, Y. Xiong, X. Yang, A.M. Castleberry, R.A. Hall, J. Biol. Chem. 281 (2006) 2820.
[22] T. Virag, D.B. Elrod, K. Liliom, V.M. Sardar, A.L. Parrill, K. Yokoyama, G. Durgam, W. Deng, D.D. Miller, G. Tigyi, Mol. Pharmacol. 63 (2003) 1032.
[23] C.C. Yun, Y. Chen, F. Lang, J. Biol. Chem. 277 (2002) 7676.
[24] X.D. Ren, M.A. Schwartz, Methods Enzymol. 325 (2000) 264.
[25] J. Xu, M. Paquet, A.G. Lau, J.D. Wood, C.A. Ross, R.A. Hall, J. Biol. Chem. 276 (2001) 41310.
[26] R.T. Terry-Lorenzo, L.C. Carmody, J.W. Voltz, J.H. Connor, S. Li, F.D. Smith, S.L. Milgram, R.J. Colbran, S. Shenolikar, J. Biol. Chem. 277 (2002) 27716.
[27] Y. Wu, D. Dowbenko, S. Spencer, R. Laura, J. Lee, Q. Gu, L.A. Lasky, J. Biol. Chem. 275 (2000) 21477.
[28] J.D. Wood, J. Yuan, R.L. Margolis, V. Colomer, K. Duan, J. Kushi, Z. Kaminsky, J.J. Kleiderlein, A.H. Sharp, C.A. Ross, Mol. Cell. Neurosci. 11 (1998) 149.
[29] H. Nakanishi, H. Obaishi, A. Satoh, M. Wada, K. Mandai, K. Satoh, H. Nishioka, Y. Matsuura, A. Mizoguchi, Y. Takai, J. Cell Biol. 139 (1997) 951.
[30] K. Adamsky, K. Arnold, H. Sabanay, E. Peles, J. Cell Sci. 116 (2003) 1279.
[31] O. Kranenburg, M. Poland, F.P.G. van Horck, D. Drechsel, A. Hall, W.H. Moolenaar, Mol. Biol. Cell 10 (1999) 1851.
[32] J. Xu, Y.-J. Lai, W.-C. Lin, F.-T. Lin, J. Biol. Chem. 279 (2004) 10459.
[33] S. Lehtonen, J.J. Ryan, K. Kudlicka, N. Iino, H. Zhou, M.G. Farquhar, Proc. Natl. Acad. Sci. U. S. A. 102 (2005) 9814.
[34] J.L. Franklin, K. Yoshiura, P.J. Dempsey, G. Bogatcheva1, L. Jeyakumar, K.S. Meise, R.S. Pearsall, D. Threadgill, R.J. Coffey, Exp. Cell Res. 303 (2005) 457.
[35] R. Yao, Y. Natsume, T. Noda, Oncogene 23 (2004) 6023.
[36] N. Suzuki, S. Nakamura, H. Mano, T. Kozasa, Proc. Natl. Acad. Sci. U. S. A. 100 (2003) 733.
[37] H. Chikumi, J. Vazquez-Prado, J.-M. Servitja, H. Miyazaki, J.S. Gutkind, J. Biol. Chem. 277 (2002) 27130.
[38] M.D. Rochdi, V. Watier, C. La Madeleine, H. Nakata, T. Kozasa, J.L. Parent, J. Biol. Chem. 277 (2002) 40751.
[39] D. Shida, T. Watanabe, J. Aoki, K. Hama, J. Kitayama, H. Sonoda, Y. Kishi, H. Yamaguchi, S. Sasaki, A. Sako, T. Konishi, H. Arai, H. Nagawa, Lab. Invest. 84 (2004) 1352.
[40] X. Fang, D. Gaudette, T. Furui, M. Mao, V. Estrella, A. Eder, T. Pustilnik, T. Sasagawa, R. Lapushin, S. Yu, R.B. Jaffe, J.R. Wiener, J.R. Erickson, G.B. Mills, Ann. N. Y. Acad. Sci. 905 (2000) 188.
[41] M.C. Huang, H.Y. Lee, C.C. Yeh, Y. Kong, C.J. Zaloudek, E.J. Goetzl, Oncogene 23 (2004) 122.